JOURNAL OF SPACECRAFT AND ROCKETS
Vol. 36, No. 5, September–October 1999

Analysis of Pressure Measurements During Cold-Gas Thruster Firings Onboard Suborbital Spacecraft

Nikos A. Gatsonis*
Worcester Polytechnic Institute, Worcester, Massachusetts 01609
and
R. E. Erlandson,† P. K. Swaminathan,† and C. K. Kumar‡
Johns Hopkins University, Applied Physics Laboratory, Laurel, Maryland 20723

Pressure measurements taken onboard a suborbital spacecraft exhibit nonperiodic pulses during attitude-control thruster firings. The attitude-control system located at the base of the conical spacecraft included eight cold-gas thrusters. The pitch and yaw thrusters delivered 1.245 N thrust while the roll thrusters delivered 3.278 N with impulses that lasted up to 0.03 s. The pressure sensor was housed inside the spacecraft on a plane 0.15 m from its base and was connected to the outside with a 0.1-m long, 0.022-m-diam tube. Analysis shows that pressure pulses appear instantaneously with firings although the thrusters did not have a direct line of sight with the sensor entrance. Pressure pulses are superimposed on a background pressure that is attributed to internal outgassing. Plumes from thrusters with the same level of thrust result in large differences in pressure depending on their orientation with respect to the entrance of the pressure-sensor tube. Data analysis demonstrates that outgassing, plume backflow, and plume/surface interaction affect the neutral pressure environment of the small suborbital vehicle.

Nomenclature

D_e = exit diameter of nozzle, mm
D_t = diameter of pressure-sensor tube, m
D_{th} = throat diameter of nozzle, mm
L_t = length of pressure-sensor tube, m
n_∞ = freestream number density, m^{-3}
T_∞ = freestream temperature, K
V_∞ = freestream velocity, m/s
λ_∞ = freestream mean-free path, m

Introduction

THE study of plumes from small attitude-control thrusters is very important for the assessment of possible spacecraft contamination, as well as for determining plume-impingement forces. There have been numerous ground-based experimental investigations of small thruster plumes.[1–3] Numerical simulation studies of plumes have been carried out with Navier–Stokes codes[4] and the direct simulation Monte Carlo (DSMC) method.[5–7] Recent plume studies combine the two methods by following the flow via a Navier–Stokes approach until breakdown is established, then continue with the DSMC approach.[8–10] Whereas numerical studies have been numerous, space-based experiments with thrusters have been limited and mostly related to the Space Shuttle. Since the early Shuttle flights, ample evidence has been provided to demonstrate the effects of thruster firings on the induced environment.[11] Many subsequent investigations have addressed the plasma, neutral, and electromagnetic environment during thruster firings.[12–14] However, the complexity of the Shuttle operations, its geometry, and its induced environment make the interpretation of neutral environment parameters very difficult. Data from rocket experiments have also demonstrated the effects of thruster firings on the neutral pressure environment.[15] Cold-gas thruster plumes have also been the subject of a recent investigation onboard Mir.[16]

Received 15 September 1998; revision received 2 March 1999; accepted for publication 30 March 1999.

*Assistant Professor, Computational Gas and Plasma Dynamics Laboratory, Mechanical Engineering Department, 100 Institute Road. Senior Member AIAA.
†Senior Professional Staff. Member AIAA.
‡Research Consultant.

This study presents data analysis of pressure measurements taken onboard a small suborbital spacecraft, the Environmental Monitor Package (EMP). The data were obtained during thruster firings of the N_2 cold-gas attitude-control system of the conical EMP spacecraft. Even with the simple geometry of the EMP, data interpretation is difficult because of outgassing from internal surfaces, complex plume/surface interactions, as well as the rarefaction effects of the plume flow entering the pressure sensor. The sensor was housed inside the EMP and was connected to the outside with a 0.1-m-long, 0.022-m-diam tube. In our previous study we studied the response of the pressure sensor and its connecting tube to the incoming flow during the quiet-thruster period while the EMP descended from an altitude of 560 km until reentry at 130 km.[17] The current investigation focuses on the thruster-firing period of the mission and presents data analysis that reveals internal outgassing, plume backflow, and plume/surface interaction phenomena. Numerical simulations of the EMP nozzle and plume flows as well as data comparisons are presented by Gatsonis et al.[18]

Experiment Description

An experiment to characterize the induced environment around a suborbital spacecraft was conducted by the Applied Physics Laboratory. The spacecraft, called the EMP, contained instruments designed to measure the total gas pressure, water vapor concentration, neutral and ion gas concentration and flux of dust particles. Figure 1 shows a schematic of the EMP spacecraft along with the location of the neutral mass spectrometer, the ion mass spectrometer, and the ionization pressure sensor.

The EMP spacecraft, containing the suite of instruments, a telemetry system, and the attitude-control system, was launched into a suborbital trajectory after its release from a postboost vehicle at 500 s (mission elapsed time) and an altitude of approximately 1000 km. The EMP reached its apogee at 840 s and an altitude of 1230 km and reentered at 1630 s and an altitude of 130 km. The approximate altitude and speed of the EMP are shown in Fig. 2. The EMP was rotating with a period of 10 s (0.1 Hz) in the direction shown in Fig. 3 throughout the mission.

The attitude-control system of the EMP, shown in Fig. 3, was located at the bottom of the conical structure and included eight thrusters: pitch-down (P-D), pitch-up (P-U), yaw-right (Y-R), yaw-left (Y-L), two roll-clockwise (R-CW_1, R-CW_2), and two roll-counterclockwise (R-CCW_1, R-CCW_2). All nozzles were conical with a 15-deg half-angle, and their characteristics are described in

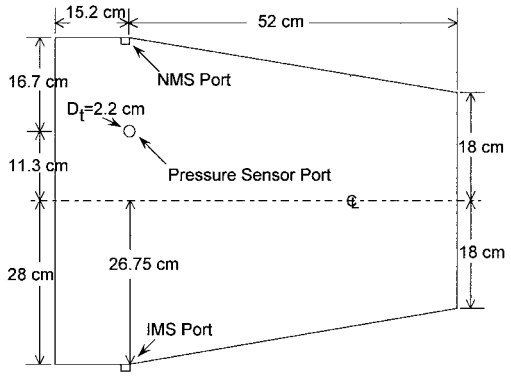

Fig. 1 EMP spacecraft geometry and instrument location.

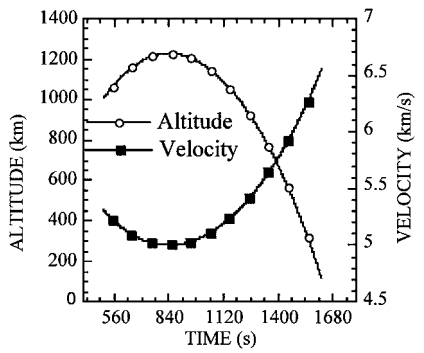

Fig. 2 EMP approximate altitude and speed.

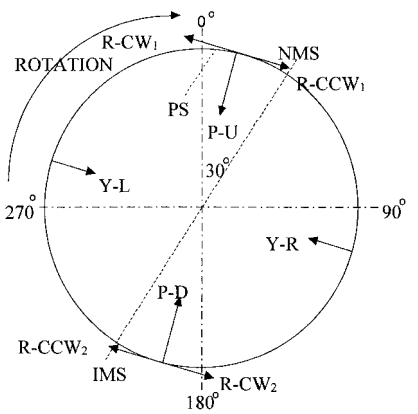

Fig. 3 Approximate thruster location on the EMP base (looking forward).

Table 1. Pressure to the solenoid valve of the nozzles was provided at 1034.25 kPa. A typical EMP thruster firing consisted of multiple impulses of 0.03 s each.

A cold-cathode ionization sensor measured the neutral gas pressure of the EMP environment. The operating range of the sensor was from 4×10^{-5} to 0.1333 Pa, and the absolute values are expected to be correct within 15% for the entire range. Pressure was sampled at a rate of 16.67 samples/s (every 0.06 s). The pressure sensor itself was housed inside the spacecraft and was connected to the entrance hole on the surface by a tube with length $L_t = 0.1$ m and diameter $D_t = 0.022$ m. The pressure tube was located approximately 0.11 m off the axis at a plane 0.15 m from the base of the spacecraft as shown in Fig. 1.

Data Analysis

Pressure was sampled by the EMP sensor at a rate of 16.67 samples/s (or every 0.06 s) while the intermittent thruster impulses lasted up to 0.03 s with each firing containing multiple impulses. The pressure data were interpolated to 0.03-s intervals and are shown in Fig. 4 for the entire EMP flight from 500 to 1630 s. This data set can be clearly divided into two periods. The first period from 500 s (1000 km) to 1400 s (670 km) exhibits nonperiodic pressure pulses with large pressure peaks that coincide with the EMP thruster firings. At approximately 1400 s the N_2 gas was depleted, and the pressure

Table 1 EMP thruster characteristics

Thruster	Thrust, N	Exit diameter D_e, mm	Throat diameter D_{th}, mm
P-U, P-D	1.245	4.826	0.906
Y-R, Y-L	1.245	4.826	0.906
R-CW, R-CCW	3.278	5.588	1.6

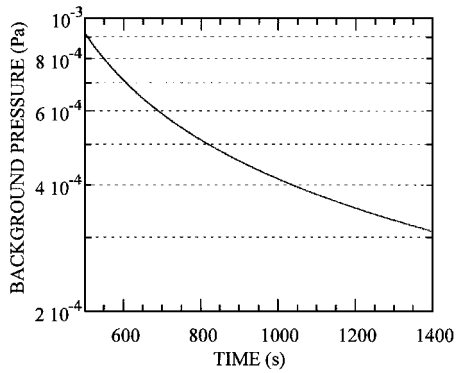

Fig. 5 Background pressure caused by outgassing during the EMP thruster firing period (500–1400 s).

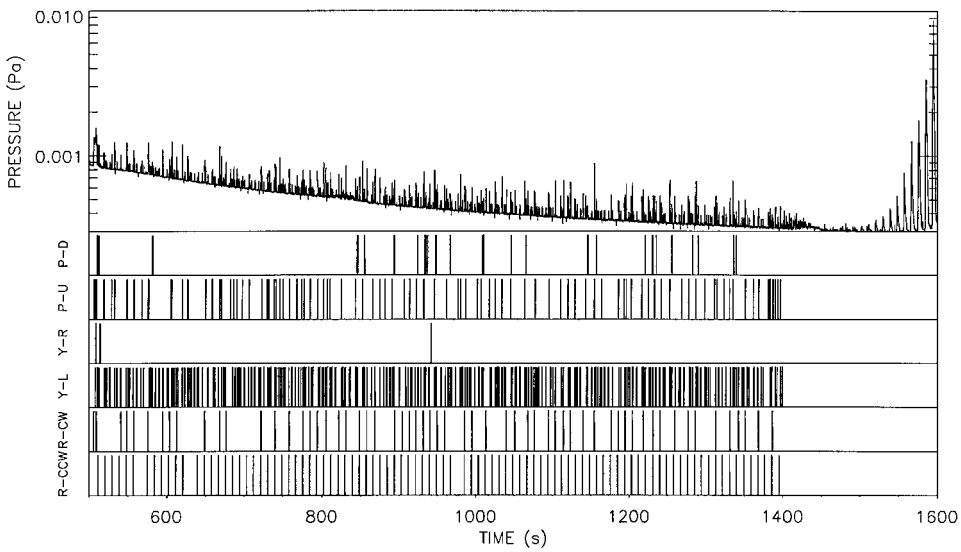

Fig. 4 Pressure data during the EMP thruster firing period (500–1400 s) and the ram-wake period (1460–1600 s).

pulses disappeared. The second period, from 1450 s (560 km) to 1630 s (130 km), shows periodic pulses related to ram-wake effects. These periodic pressure pulses coincide with the EMP period of rotation and increase in amplitude as the EMP descended to lower altitudes and higher freestream densities. The analysis of the ram-wake period and the response of the pressure sensor to the incoming flow were the subject of our previous investigation.[17]

Background Pressure Caused by Outgassing

The first obvious trend shown in Fig. 4 is that pressure pulses are superimposed on a background that gradually decreases as the mission time increases. This background pressure is approximately 9×10^{-3} Pa at the beginning of the flight and reduces to 3×10^{-4} Pa at 1400 s. Ambient data based on the MSIS-86 model for three characteristic altitudes during the EMP thruster-firing period are shown in Table 2. Estimates of the ambient pressure, the incident pressure to the EMP, and the measured background pressure are also presented in Table 2 for comparison. The EMP was flying at altitudes above 670 km during the thruster-firing period, and the background pressure is several orders of magnitude larger than both the ambient and incident pressure as indicated by Table 2. This background pressure can, therefore, be attributed to the internal outgassing of the spacecraft and sensor surfaces. This behavior has also been observed in recent suborbital rocket experiments.[15]

To obtain the background pressure from the data, we used the following noise construction algorithm. The first 500 data points from the entire data set were sorted and a least-squares fit was performed for the 30 points with the lowest values. This fit was extended to cover the entire 500-data window and was assumed to represent the background pressure for that time period. The procedure was repeated for the next 500 data points until the entire data set was covered. A plot of the background pressure caused by outgassing is shown in Fig. 5.

Reduced Pressure Induced by Thruster Plumes

To obtain the pressure associated with thruster firings, the background pressure caused by outgassing was subtracted from measurements, and the result was designated as the reduced pressure. The pressure, reduced pressure, and the associated thruster firings as a function of time are shown in Fig. 6 for the entire thruster-firing period. Expanded details of a typical pressure profile are shown in Fig. 7 for the period between 840 and 860 s. The pressure peaks and the thruster firings coincide within the temporal resolution of the sampling as Fig. 7 shows. A typical pressure peak appears instantaneously with the thruster impulse and gradually decreases. From these data one can see that although the plumes of the EMP thrusters did not have a direct line of sight with the entrance to the pressure sensor, they caused instantaneous pressure increases.

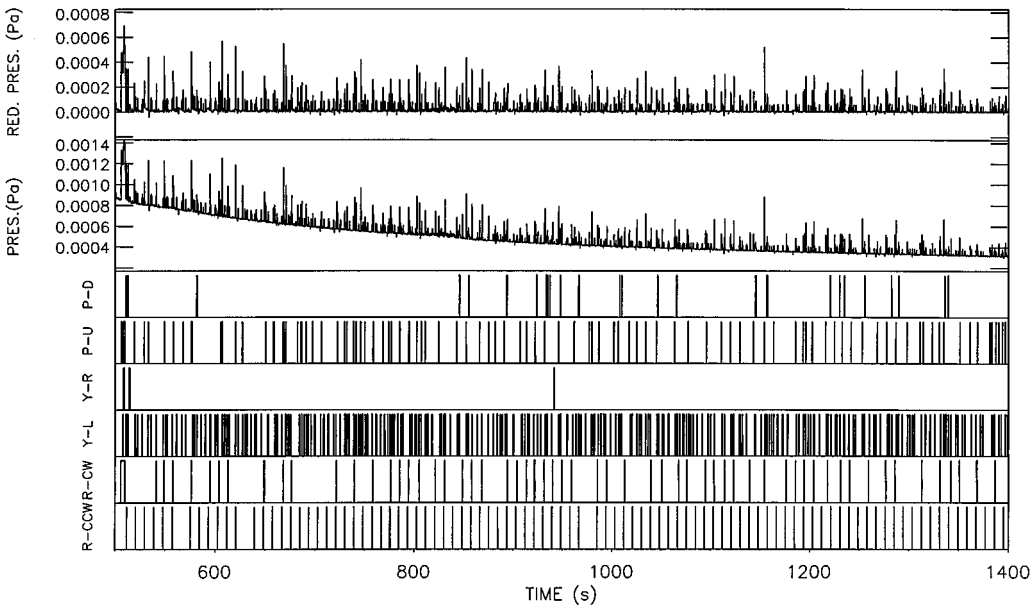

Fig. 6 Pressure, reduced pressure, and thruster impulses during the entire thruster-firing period.

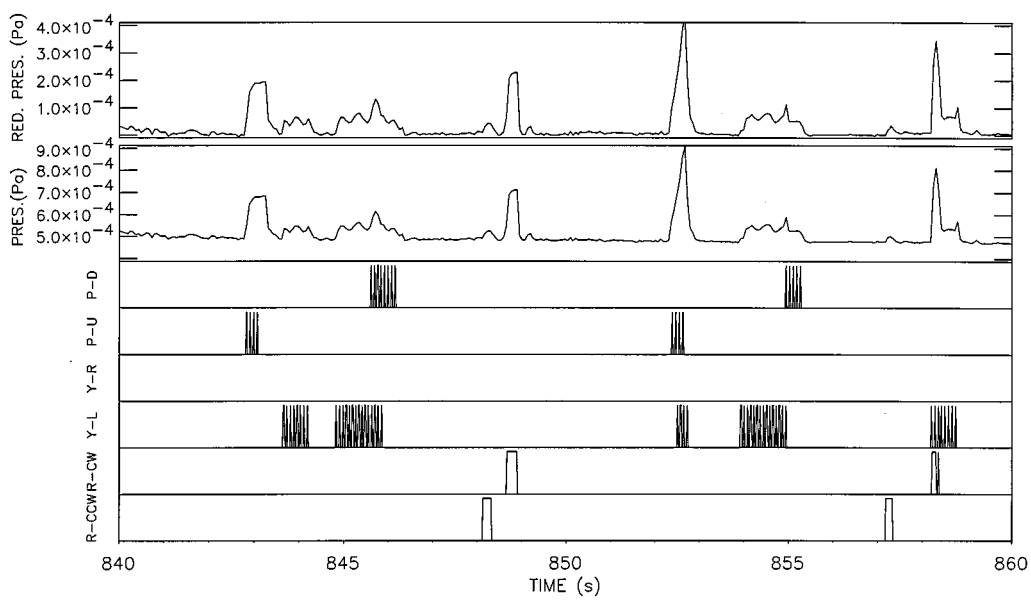

Fig. 7 Details of pressure, reduced pressure, and thruster firings for the 840–860-s period.

Table 2 Freestream parameters and pressure during the EMP thruster-firing period

Time, s	Altitude, km	n_∞, m^{-3}	T_∞, K	Mole fraction					V_∞, m/s	Ambient pressure, Pa	Incident pressure, Pa	Background pressure, Pa
				N	N_2	O	O_2	H				
500	1000	5.74×10^{11}	950	3.6×10^{-4}	3.7×10^{-7}	1.4×10^{-2}	7.3×10^{-10}	0.986	5311	6.3×10^{-9}	1.2×10^{-7}	9×10^{-3}
859	1228	2.75×10^{11}	950	5.9×10^{-5}	4.8×10^{-9}	1.6×10^{-3}	4.7×10^{-12}	0.998	5000	3.1×10^{-9}	4.9×10^{-8}	5×10^{-3}
1400	670	3.4×10^{12}	950	5.2×10^{-3}	4.9×10^{-4}	3.9×10^{-1}	3.7×10^{-6}	0.679	5770	3.7×10^{-8}	1.7×10^{-6}	3×10^{-3}

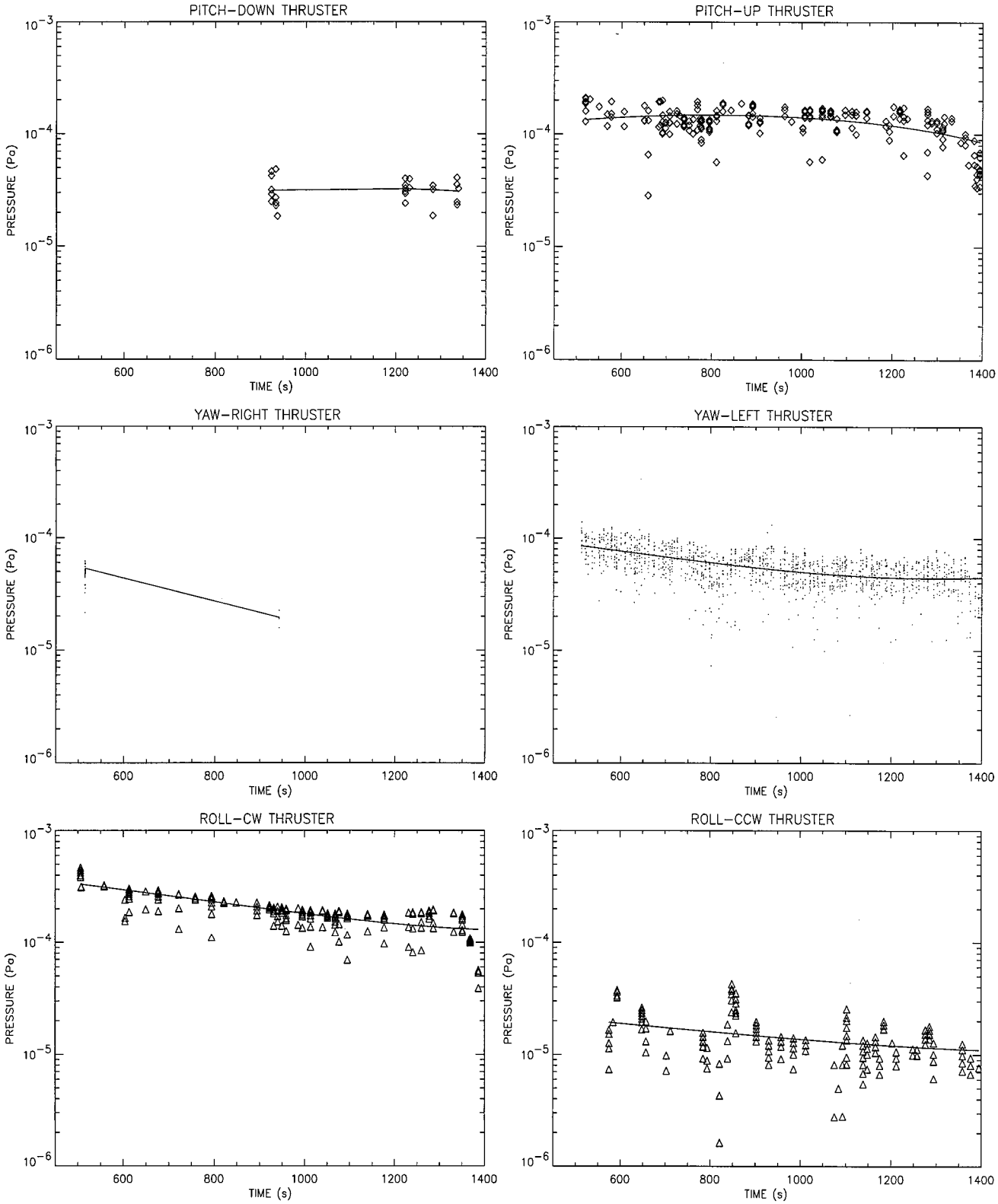

Fig. 8 Reduced pressure data for individual thruster-firing events.

Table 3 Pressure and reduced pressure of individual thrusters

Thruster (sample number)	Sample number	Pressure, Pa		Reduced pressure, Pa	
		Average	Std. dev.	Average	Std. dev.
P-D	27	4.05×10^{-4}	4.9×10^{-5}	3.19×10^{-5}	7.73×10^{-6}
P-U	210	5.89×10^{-4}	1.52×10^{-4}	1.3×10^{-4}	3.91×10^{-5}
Y-R	21	8.31×10^{-4}	1.2×10^{-4}	4.56×10^{-5}	1.34×10^{-5}
Y-L	1450	5.31×10^{-4}	1.53×10^{-4}	5.67×10^{-5}	2.04×10^{-5}
R-CW	270	7.02×10^{-4}	2.5×10^{-4}	2.09×10^{-4}	7.81×10^{-5}
R-CCW	248	4.51×10^{-4}	1.16×10^{-4}	1.41×10^{-5}	7.25×10^{-6}

During the EMP mission, finding more than one thruster firing simultaneously, as Figs. 6 and 7 show, was typical. To examine the effects of individual thrusters, the pressure resulting from single thruster-firing events was calculated. The criterion to establish a single-thruster event was that no other thruster operated 0.5 s before and 0.1 s after the firing of the thruster under investigation. Pressure measurements associated with individual thruster firings are shown in Fig. 8, and the average pressures estimated from these data are shown in Table 3. This analysis shows that thrusters with the same thrust level do not produce similar pressure effects. For example, the R-CW thrusters produced an order-of-magnitude larger pressure amplitudes than the R-CCW ones. Based on the location of the R-CCW thrusters, shown in Fig. 3, their plumes are directed away from the sensor entrance. Specifically, the R-CCW_1 plume could reach the sensor entrance because of backflow only. The R-CCW_2 plume, directed at almost 90 deg with respect to the sensor-tube centerline, could reach the entrance only after expanding on the EMP base. However, the plume from the R-CW_1 thruster could reach the sensor entrance directly after a short expansion off the EMP base, which explains the resulting higher pressure. In contrast, differences between the yaw thrusters are relatively small, which can be attributed to the almost symmetric location of the yaw thrusters with respect to the pressure-sensor entrance, as shown in Fig. 3. Note that the yaw plumes could reach the sensor entrance after expanding on the EMP base. The P-D thruster located at the opposite side of the pressure-sensor entrance resulted in a smaller pressure compared to the P-U. Note that backflow is the only way for the P-U thruster plume to reach the pressure-sensor entrance. The P-D thruster plume expanding on the EMP base could reach the entrance only by wrapping around the EMP side surface. All of the precedings suggest that plume backflow, plume wrap-around, and plume/surface interactions are responsible for the observed EMP pressure environment.

Conclusion

Data analysis of pressure measurements obtained from a cold-cathode ionization sensor onboard the EMP suborbital spacecraft was presented. The data, collected during firings of small attitude-control thrusters, revealed plume backflow and plume/surface interaction. The plumes from the EMP thrusters did not have a direct line of sight with the pressure-sensor entrance but caused instantaneous pressure peaks upon their firing. The analysis revealed that outgassing from internal surfaces resulted in a background pressure that decreased with time. Analysis of individual thrusters showed that firings resulted in pressure peaks that depended upon the thruster location on the base of the EMP. Our analysis demonstrated that plume/surface interactions and backflow contributed to the EMP pressure environment.

Acknowledgment

The authors would like to thank S. Wing for assistance in data analysis.

References

[1]Dettleff, G., Boettcher, R. D., Dankert, C., Koppenwallner, G., and Legge, H., "Attitude Control Thruster Plume Flow Modeling and Experiments," *Journal of Spacecraft and Rockets*, Vol. 23, No. 5, 1986, pp. 476–481.

[2]Legge, H., and Dettleff, G., "Pitot Pressure and Heat Transfer Measurements in Hydrazine Thruster Plumes," *Journal of Spacecraft and Rockets*, Vol. 23, No. 4, 1986, pp. 357–362.

[3]Boyd, I. D., Penko, P. F., Meissner, D. L., and DeWitt, K. J., "Experimental Investigations of Low Density Nozzle and Plume Flows of Nitrogen," *AIAA Journal*, Vol. 30, No. 10, 1992, pp. 2453–2461.

[4]Gilmore, M. R., "Breakdown of Continuum Solvers in Rapidly Expanding Flows," AIAA Paper 95-2134, June 1995.

[5]Bird, G. A., *Molecular Gas Dynamics and the Direct Simulation of Gas Flows*, Clarendon, Oxford, 1994.

[6]Bird, G. A., "Breakdown of Translational and Rotational Equilibrium in Gaseous Expansions," *AIAA Journal*, Vol. 8, No. 11, 1970, pp. 1998–2003.

[7]Tartabini, P. V., Wilmoth, R. G., and Rault, D. F. G., "Direct Simulation Monte Carlo Calculation of a Jet Interaction Experiment," *Journal of Spacecraft and Rockets*, Vol. 32, No. 1, 1995, pp. 75–83.

[8]Rault, D. F. G., "Methodology for Thruster Plume Simulation and Impingement Effects Characterized Using DSMC," AIAA Paper 95-2032, June 1995.

[9]Lumpkin III, F. E., Stuart, P. C., and LeBeau, G. J., "Enhanced Analysis of Plume Impingement During Shuttle-Mir Docking Using a Combined CFD and DSMC Methodology," AIAA Paper 96-1877, June 1996.

[10]Ivanov, M. S., Markelov, G. N., Kashkovsky, A. V., and Giordano, D., "Numerical Analysis of Thruster Plume Interaction Problems," *Proceedings of the 2nd European Spacecraft Propulsion Conference*, ESA, Noordwijk, The Netherlands, 1997, pp. 603–610.

[11]Carignan, G. R., and Miller, E. M., "Mass Spectrometer," *STS-2, -3, -4 Induced Environment Contamination Monitor (IECM)*, edited by E. R. Miller, NASA TM-82524, 1983, pp. 87–101.

[12]Wulf, E., and Von Zahn, U., "The Shuttle Environment: Effects of Thruster Firings on Gas Density and Composition in the Payload Bay," *Journal of Geophysical Research-Space Physics*, Vol. 91, No. A3, 1986, pp. 3270–3278.

[13]Grebowsky, J. M., Taylor, H. A., and Pharo, M. W., "Thermal Ion Perturbations Observed in the Vicinity of the Space Shuttle," *Planetary Space Science*, Vol. 35, No. 4, 1987, pp. 501–513.

[14]Gatsonis, N. A., and Hastings, D. E., "Evolution of the Plasma Environment Induced by Gas Releases from Spacecraft: Three-Dimensional Modeling," *Journal of Geophysical Research-Space Physics*, Vol. 97, No. A10, 1992, pp. 14980–15005.

[15]Pickett, J. S., Morgan, D. D., and Merlino, R. L., "Payload Environment and Gas Release Effects on Sounding Rocket Neutral Pressure Measurements," *Journal of Spacecraft and Rockets*, Vol. 33, No. 4, 1996, pp. 501–506.

[16]Ivanov, M. S., Markelov, G. N., Gerasimov, Yu. I., Krylov, A. N., Mishina, L. V., and Sokolov, E. I., "Free-Flight Experiment and Numerical Simulation for Cold Thruster Plume," AIAA Paper 98-0898, Jan. 1998.

[17]Gatsonis, N. A., Maynard, E. P., and Erlandson, R. E., "Monte Carlo Modeling and Analysis of Pressure Sensor Measurements During Suborbital Flight," *Journal of Spacecraft and Rockets*, Vol. 34, No. 1, 1997, pp. 83–91.

[18]Gatsonis, N. A., Nanson, R. A., and LeBeau, G. J., "Simulations of Cold-Gas Nozzle and Plume Flows and Flight Data Comparisons," *Journal of Spacecraft and Rockets* (to be published).

R. G. Wilmoth
Associate Editor